DEVELOPMENT OF OXIDE FIBROUS MONOLITH SYSTEMS*

K. C. Goretta, D. Singh, and W. A. Ellingson
Energy Technology Division
Argonne National Laboratory, Argonne, IL 60439

W. R. Kriven
Department of Materials Science and Engineering
University of Illinois, Urbana, IL 61801

J. C. McNulty and F. W. Zok
Materials Department
University of California, Santa Barbara, CA 93160

January 1999

Submitted to Proceedings of 23rd Annual Conference on Composites, Materials and Structures, Cocoa Beach, FL, January 25-28, 1999.

*Work supported by the Defense Advanced Research Projects Agency, through a Department of Energy Interagency Agreement, under Contract W-31-109-Eng-38.

DISCLAIMER

DISCLAIMER

Portions of this document may be illegible in electronic image products. Images are produced from the best available original document.

DEVELOPMENT OF OXIDE FIBROUS MONOLITH SYSTEMS

K. C. Goretta, D. Singh, and W. A. Ellingson
Energy Technology Division
Argonne National Laboratory, Argonne, IL 60439

W. M. Kriven
Department of Materials Science and Engineering
University of Illinois, Urbana, IL 61801

J. C. McNulty and F. W. Zok
Materials Department
University of California, Santa Barbara, CA 93160

INTRODUCTION

Fibrous monolithic ceramics generally have a cellular structure that consists of a strong cell surrounded by a weaker boundary phase [1-5]. Fibrous monoliths (FMs) are produced from powders by conventional ceramic fabrication techniques, such as extrusion [1,2]. When properly engineered, they exhibit fail gracefully [3-5].

Several compositions of ceramics and cermets have been processed successfully in fibrous monolithic form [4]. The most thoroughly investigated fibrous monolith consists of Si_3N_4 cells and a BN cell-boundary phase [3-5]. Through appropriate selection of initial powders and extrusion and hot-pressing parameters, very tough final products have been produced. The resultant high toughness is due primarily to delamination during fracture along textured platelike BN grains.

The primary objectives of our program are to develop:

1. Oxide-based FMs, including new systems with improved properties.
2. FMs that can be pressureless sintered rather than hot-pressed.
3. Techniques for continuous extrusion of FM filaments, including solid freeform fabrication (SFF) for net-shape fabrication of FMs.
4. Predictive micromechanical models for FM design and performance.
5. Ties with industrial producers and users of FMs._

OXIDE FIBROUS MONOLITHS

Oxides are, of course, stable in air and thus offer an advantage over structural ceramics such as SiC and Si_3N_4. In continuous-fiber ceramic composites, oxides with tailored matrix-phase porosity have achieved excellent fracture toughnesses [6]. For FM systems, the goal is to promote delamination along the cell/boundary interface, which will lead to a large work of fracture [3-5,7]. Tailored porosity is one possible way to achieve this goal. Interphases, such as $LaPO_4$ [8] and YPO_4 [9], can also promote the required delamination.

Use of oxides that exhibit phase transformations is also being examined. Transformations that induce reductions in unit-cell volume should promote delamination in the interphase. Such transformations, which can occur in oxides over a wide temperature range (Table I), open up the possibility of tailoring oxide FMs to application temperatures [10]. Our goal is to develop FMs from at least some of the systems shown in Table I.

Table I. Oxide systems that exhibit phase transformations with volume decreases; transformation temperature is denoted T_0.

Compound	Crystal structures	T_0 (°C)	Vol. change (%)
$MgSiO_3$	Orthorhombic → monoclinic	865	–5.5
$YNbO_4$	Tetragonal → monoclinic	900	–1.8
$LnBO_3$ (type)	Hexagonal → hexagonal	550–800	–8.2
SiO_2	Cubic → tetragonal	265	–2.8
$BaAl_2Si_2O_8$	Hexagonal → orthorhombic	300	–0.43
$KAlSi_2O_6$	Cubic → tetragonal	620	≈0

SINTERED FIBROUS MONOLITHS

Sintering offers clear advantages over hot-pressing in terms of cost and range of parts that can be produced. Sintering of multiphase ceramics requires, however, matching sufficiently well both firing shrinkage and thermal contraction upon cooling [11,12]. Multilayer oxides are routinely produced by controlling the distribution of powder particle size, the concentration and type of combustible phase and possible sintering aids, the and heat-treatment conditions. In the sintering effort, we are examining primarily oxides, but are also interested in materials such as Si_3N_4/BN. We are using highly sinterable oxide powders, with fine particle size and high specific surface area, that can be made at reasonable cost by a recently developed complexation-polymerization method [13-15].

Efforts to date suggest that the density of a particular phase has little effect on its thermal-expansion coefficient (Fig. 1). Therefore, the key considerations for producing robust FMs are matching of shrinkage and phase assemblage. For FMs of a single basic constituent, such as dense, strong mullite cells with porous, weaker mullite cell boundaries, only shrinkage need be matched, which can be accomplished by, for example, adding carbon powder to the cell-boundary mixture.

For multiphase FMs, thermal-expansion coefficients can be tailored to a certain extent by controlling texture or by adding phases of higher or lower thermal expansion. There is a limit on the extent to which thermal-expansion coefficients can be controlled, but the ranges of thermal-expansion coefficients of useful structural oxides and nonoxides is large, and many blends are possible.

FABRICATION OF FM COMPONENTS

Most FM components are now fabricated from billets that consist of a core and sheath [2-5]. In our work, we seek to produce filaments continuously. Two basic methods are available to do this. First, one can use coextrusion dies, for which individual hoppers can be supplied with the required mixes [16]. Second, one can use SFF technology. With SFF, filament can also be directly patterned into a part [17], which should reduce costs by greatly reducing handling steps. Our work actively follows both technological approaches. Our SFF work requires developing feedstock with suitable rheology and binder-burnout and sintering responses, modifying the heads of commercial units, and upgrading software. We can now extrude monofilaments through our SFF apparatus and are working on new compositions tailored to FM production.

In concert with these efforts to fabricate two-phase FMs, we are examining fabrication of three-phase FMs; i.e., FMs that contain a cell, an interphase, and a matrix (Fig. 2). The cell and interphase can be made by coextrusion; the matrix can be made by wrapping the filaments or by various infiltration techniques. This weakest phase in the three-phase structure is not continuous. Crack delamination, especially from out-of-plane loading, should therefore occur discreetly from one cell to the next, with each interphase acting as a sort of crack trap. Such a configuration should lead to greater strength and fracture toughness.

MICROMECHANICAL MODELING

FMs offer the potential for high toughness and damage tolerance, in combination with other attractive characteristics intrinsic to ceramics. Yet, the current understanding of the toughening mechanisms and the associated mechanics in FMs is rudimentary at best. Some insight has been gained through the use of out-of-plane flexure tests on laminated unidirectional and cross-ply FMs. Under these conditions, failure is accompanied by large-scale delamination between the cell plies [2-5], which is closely analogous to that of weakly bonded layered systems.

In contrast, relatively little experimental or theoretical work has been devoted to in-plane notched properties. Indeed, the in-plane properties are expected to be most relevant to the design of FM components, especially under thermal loading conditions [18]. To this end, a combined experimental and modeling program has been initiated to assess the in-plane mechanical properties of FMs, with special emphasis on notch sensitivity. The anisotropy of these properties is being probed through mechanical tests on cross-ply systems in both 0°/90° and ±45° orientations (Fig. 3).

The corresponding modeling activity, based in part on the mechanics of cohesive zones, is being developed to simulate notched behavior. Comparisons between experiment and theory will be used to assess the validity of the modeling approach, as well as to extract the material properties that are pertinent to the description of fracture resistance. Complementary micromechanical measurements are also being contemplated, including measurement of the sliding resistance of the BN interphase by use of fiber pushout tests.

Additional insight into the fracture behavior is expected to emerge from measurements and modeling of the thermal residual stresses and strains. We are using neutron diffraction to measure the residual strains directly [19,20]. BN absorbs neutrons strongly; thus, strains in BN cannot be measured with neutrons. In the Si_3N_4/BN system, the BN is very weak and the Si_3N_4 phase will control the strength, and so the most important measurements are in the Si_3N_4 phase in any case.

To date, several Si_3N_4/BN specimens from two panels of Si_3N_4/BN FMs with 0°/90° and ±45° fiber architectures have been tested at the University of California at Santa Barbara (Fig. 4). Unnotched and notched in-plane bend tests have been performed in both orientations. The unnotched specimens were instrumented with two strain gauges on each of the compressive and the tensile faces within the constant moment region. The notched specimens were instrumented with a crack mouth opening displacement (CMOD) gauge. In addition, for both notched and unnotched specimens, the load-point displacement was measured with a deflection gauge placed in contact with the specimen. The tests on the notched specimens were periodically interrupted and unloading/reloading excursions were performed. The latter measurements are being used to determine the instantaneous compliance and assess the degree of hysteresis associated with nonlinear deformation.

The unnotched specimens in the 0°/90° orientation exhibited small amounts of inelastic straining, initiating at a stress of ≈60 MPa. At the stress maximum (≈240 MPa), the inelastic tensile strain was ≈0.03%. Fracture occurred catastrophically, with a precipitous load drop

from the load maximum. Nevertheless, the specimens remained intact because of the interlocking of the broken cells.

In the ±45 orientation, nonlinearity was also observed, although the stress at the onset (≈115 MPa) was higher. Additionally, the amount of inelastic strain was somewhat higher (≈0.05%). A particularly notable difference was the stable development of damage past the load maximum in the ±45° specimens. A precipitous load drop was obtained subsequently, starting at a stress of ≈75% of the peak value, dropping to ≈15% of the peak. Despite these differences, the bending strengths in the two orientations were similar.

Scanning electron photomicrographs of broken test specimens revealed jagged fracture paths in both orientations, the effect being more pronounced in the ±45° specimens. These observations attest to the efficacy of the BN interphase in deflecting cracks. In addition, observations on the tensile face of the ±45° specimens revealed regions in which substantial sliding had occurred between neighboring cells in adjoining layers (Fig. 5).

Notched three-point and four-point specimens exhibited essentially the same properties as one another. An example of the bending response of the three-point specimens is shown in Fig. 6. In both orientations, crack growth occurred stably past the load maximum. The unloading/reloading loops revealed significant amounts of hysteresis, presumably because of the interlocking and frictional sliding between broken fibers in the crack wake. The effects of this crack-wake friction are also evidenced in remarkably small changes in specimen compliance with increasing crack growth. The work of fracture (WOF) values obtained from the notched tests were 2100 and 5700 J/m^2 for the 0°/90° and ±45° orientations, respectively. The corresponding values of steady-state fracture resistance were 21 and 33 $MPa(m)^{0.5}$, much higher than the values typical of the toughest monolithic Si_3N_4, ≈8 $MPa(m)^{0.5}$.

Photomicrographs of the fracture surfaces of the notched specimens are shown in Fig. 7. The notable effect of fiber architecture is the more tortuous crack path and the greater amount of pullout in the ±45° specimens. Such effects are likely to be responsible for the higher values of WOF and the enhanced stability of the cracks in the ±45° orientation.

Preliminary calculations based on linear elastic fracture mechanics have revealed significant discrepancies between the predicted and measured load-CMOD and compliance-CMOD responses, highlighting the need for alternative modeling approaches. To this end, approaches that incorporate nonlinear deformation effects during crack growth, such as those based on cohesive zones models, are being developed and evaluated.

At Argonne National Laboratory, we are working to expand nondestructive examination of FMs. This effort is essential to the modeling program, both to ensure specimen quality and provide baseline data such as elastic moduli [21], and, ultimately, to ensure the quality and reproducibility of manufacturing operations. We are using acoustic, thermal, and X-ray techniques to identify flaws (Fig. 8), acoustic and optical techniques to determine elastic moduli, and various techniques to examine green filament characteristics [22,23]. For example, we have developed an impulse-excitation technique for measuring the elastic modulus of BN.

The results of the experimental and modeling work are expected to provide the knowledge base necessary for rational design of FM components, taking proper account of nonlinear damage and deformation in the description of fracture resistance, including scale effects. In addition, by identifying the material properties that enhance fracture resistance, strategies for tailoring the chemistry and microstructure of the FMs may emerge and thereby assist material development activities elsewhere in this program.

INDUSTRIAL COLLABORATIONS

Our program is focused on developing oxide FMs for low-stress applications at ≤1200°C. We are pursuing several applications, such as components in diesel or turbine engines.

SUMMARY

Our program to develop FM technology consists of several projects. Focus is centered on oxides for use at ≤1200°C, but nonoxides for use at higher temperatures are also being examined. To reduce costs and expand the range of parts that can be produced, we are developing sinterable compositions and continuous extrusion technologies, such as SFF. Micromechanical modeling and testing efforts will replace the current, largely trial-and-error, approach to design of FM materials and components with effective quantitative models. Extensive testing should verify the validity of the models. The main goal of our effort is to produce robust, reliable parts with predictable properties that can be used in a range of applications.

ACKNOWLEDGMENTS

We thank Advanced Ceramics Research for providing the Si_3N_4/BN fibrous monoliths and BN plate, and L. P. Zawada of Wright-Patterson Air Force Base and J. Finch of the University of Dayton Research Institute for providing some of the NDE data. This work was supported by the Defense Advanced Research Projects Agency, through a Department of Energy Interagency Agreement, under Contract W-31-109-Eng-38 at Argonne and through subcontracts to the universities.

REFERENCES

1. W. S. Coblenz, U.S. Patent 4,772,524, Sept. 20, 1988.
2. D. Popovic', J. W. Halloran, G. E. Hilmas, G. A. Brady, S. Somas, A. Bard, and G. Zywicki, U. S. Patent 5,645,781, July 8, 1997.
3. G. Hilmas, G. A. Brady, U. Abdali, G. Zywicki, and J. Halloran, Mater. Sci. Eng. **A195**, 263 (1995).
4. D. Kovar, B. H. King, R. W. Trice, and J. W. Halloran, J. Am. Ceram. Soc. **80**, 2471 (1997).
5. D. Popovich, G. A. Danko, G. E. Hilmas, K. Stuffle, B. H. King, G. A. Brady, R. W. Trice, and J. W. Halloran, Ceram. Eng. Sci. Proc. **17** [3], 278 (1996).
6. C. G. Levi, J. Y. Yang, B. J. Dalgleish, F. W. Zok, and A. G. Evans, J. Am. Ceram. Soc. **81**, 2077 (1998).
7. P. E. D. Morgan and D. B. Marshall, Mater. Sci. Eng. **A162**, 15 (1993).
8. P. E. D. Morgan, D. B. Marshall, and R. M. Housley, Mater. Sci. Eng. **A195**, 215 (1995).
9. D.-H. Kuo and W. M. Kriven, Mater. Sci. Eng. **A241**, 241 (1998).
10. W. M. Kriven, J. de Phys. IV [Coll. 8] **5**, 101 (1995).
11. S. J. Lee and W. M. Kriven, Ceram. Eng. Sci. Proc. **19** [3], 305 (1998).
12. M. T. Lanagan, S. E. Dorris, J. P. Singh, K. C. Goretta, U. Balachandran, C. A. Youngdahl, J. T. Dusek, J. J. Picciolo, and R. B. Poeppel, J. Met. **42** [6], 16 (1990).
13. M. A. Gulgun and W. M. Kriven, Ceram. Trans. **62**, 57 (1995).
14. S. J. Lee and W. M. Kriven, Ceram. Eng. Sci. Proc. **19** [3], 305 (1998).
15. S. J. Lee and W. M. Kriven, J. Amer. Ceram. Soc. **81**, 2605 (1998).
16. B. J. Polzin, T. A. Cruse, D. Singh, J. J. Picciolo, J. T. Dusek, M. Tlustochowicz, and K. C. Goretta, these proceedings.
17. S. Pekin, A. Zangvil, and W. Ellingson, to be published in the Proc. of Ninth Solid Freeform Fabrication Conference, Austin, TX, 1998
18. L. P. Zawada, Ceram. Eng. Sci. Proc. **19** [3], 327 (1998).
19. S. Majumdar, D. Kupperman, and J. Singh, J. Am. Ceram. Soc. **71**, 858 (1988).

20. A. Saigal, D. S. Kupperman, J. P. Singh, D. Singh, J. Richardson, and R. T. Bhatt, Comp. Eng. **3**, 1075 (1993).
21. R. Bemis, K. Shiloh, and W. Ellingson, Trans. ASME, J. Eng. Gas Turb. Power **118**, 491 (1996).
22. S. Ahuja, W. A. Ellingson, J. S. Steckenrider, and S. King, in *Thermal Conductivity 23*, eds. K. E. Wilkes, R. B. Dindiddie, and R. S. Graves (Technomic, Lancaster, PA, 1996) p. 311.
23. E. A. Sivers, W. A. Ellingson, S. A. Snyder, and D. A. Holloway, Trans. ASME, J. Eng. Gas Turb. Power **118**, 711 (1996).
24. J. Finch and L. P. Zawada, communication to W. A. Ellingson (1997).

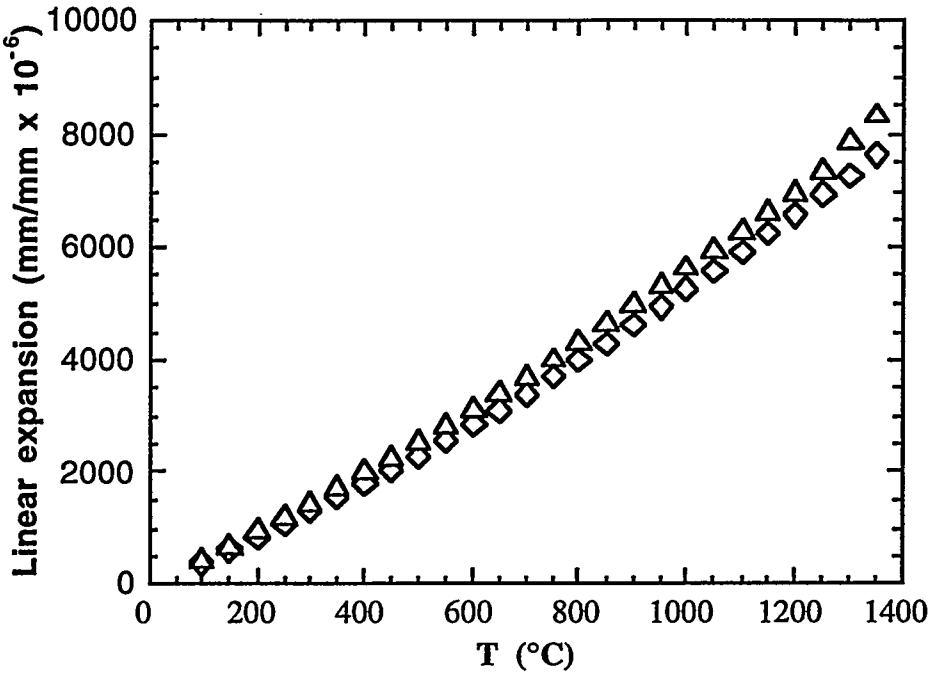

Fig. 1. Thermal-expansion data for mullite in air, with 300°C/h heating and cooling rates; triangles = 96% dense and diamonds = ≈70% dense.

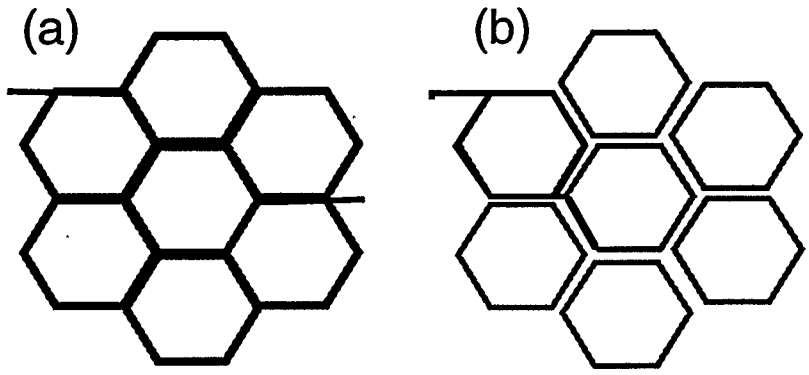

Fig. 2. Schematic diagram of (a) crack propagating through conventional FM and (b) crack propagating partially through a three-phase FM with weak interphase.

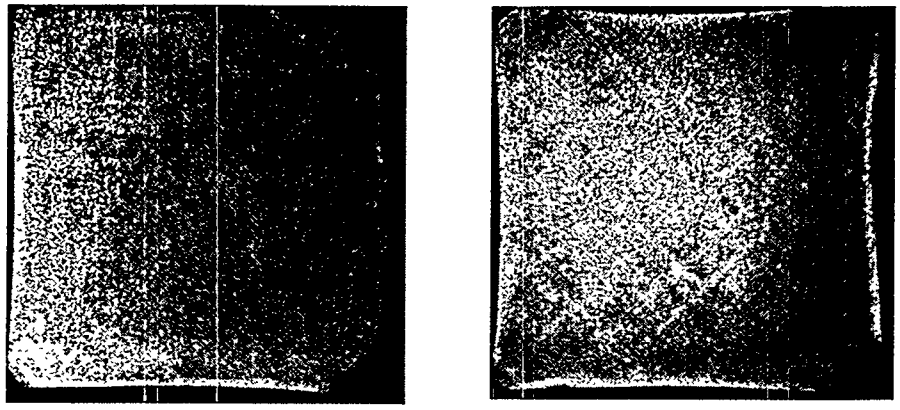

(a) (b)

Fig. 3. Through-thickness X-ray images of (a) 0°/90° and (b) ±45° Si_3N_4/BN FM; each plate is ≈150 mm wide and exhibits excellent uniformity.

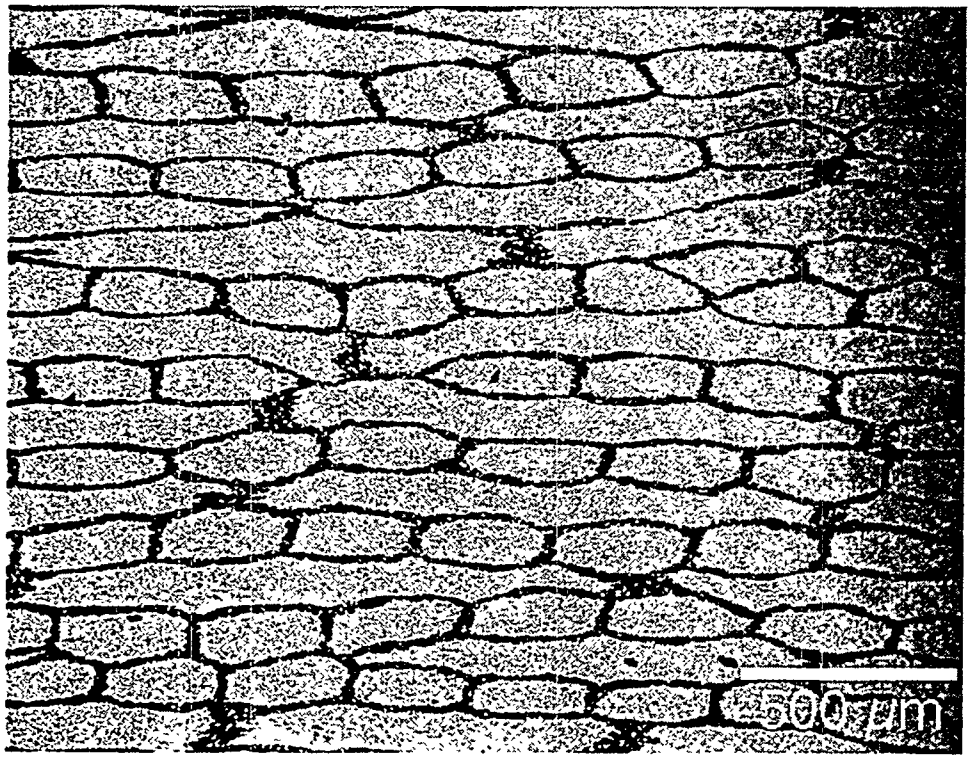

Fig. 4. Scanning electron photomicrograph of 0°/90° Si_3N_4/BN FM.

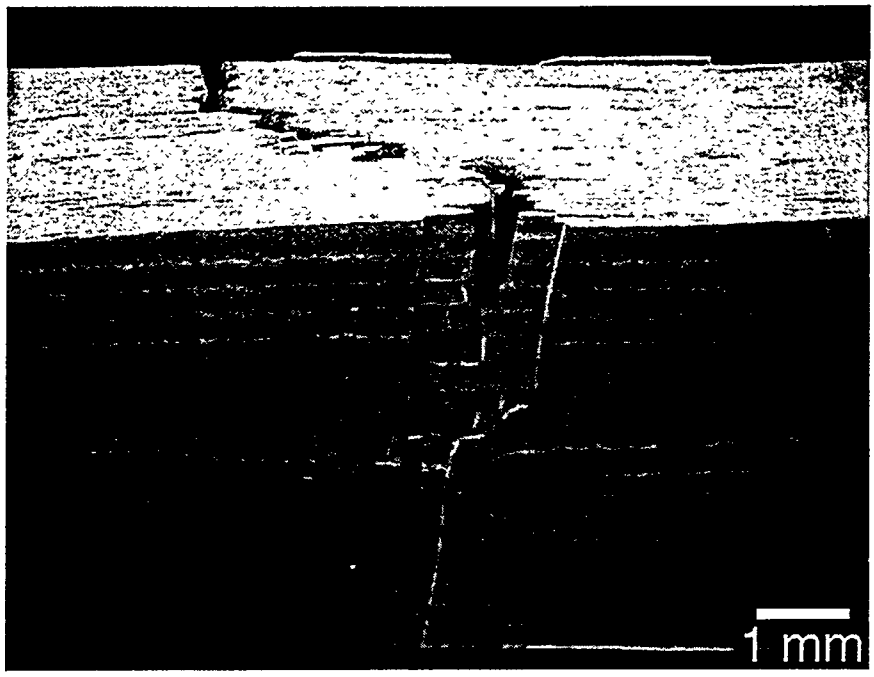

(a)

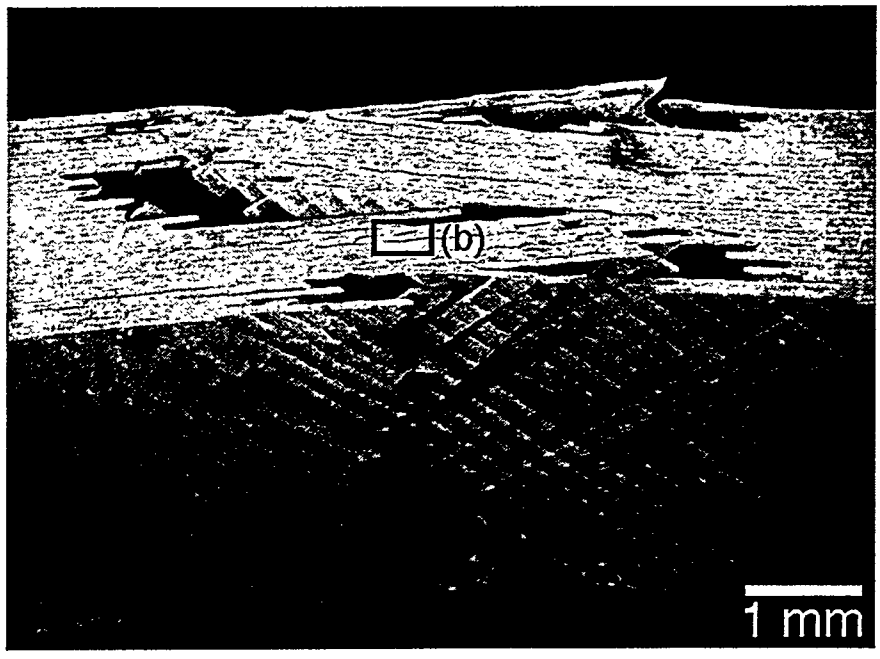

(b)

Fig. 5. Scanning electron photomicrographs of fracture in unnotched (a) 0°/90° and (b) ±45° Si_3N_4/BN laminate; box region in (b) showed substantial sliding of fibrous cells.

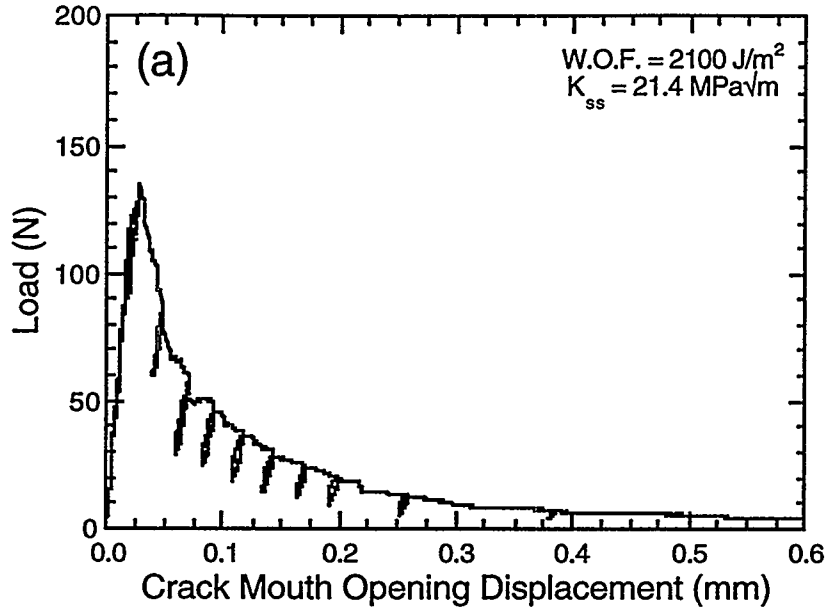

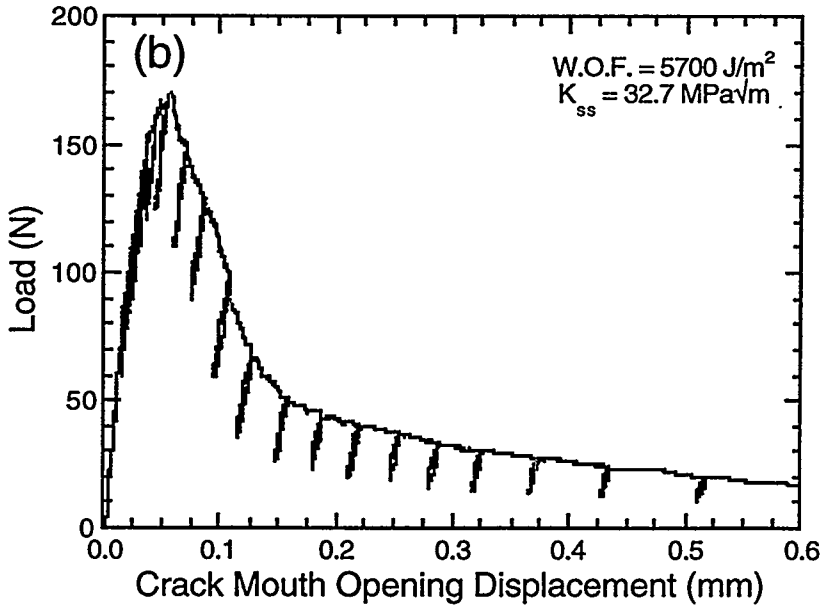

Fig. 6. Bending response of notched (a) 0°/90° and (b) ±45° Si_3N_4/BN specimens.

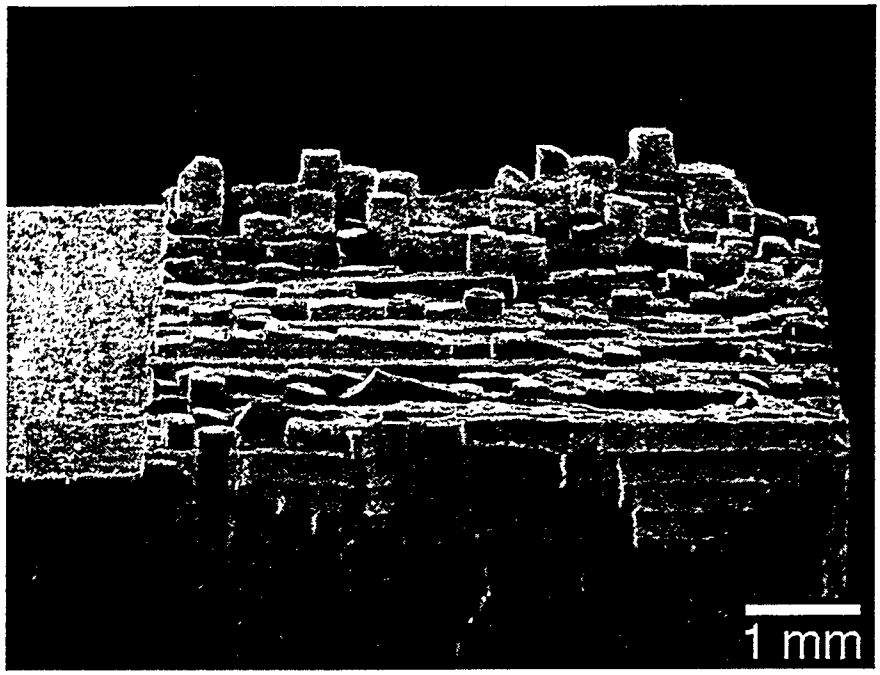

(a)

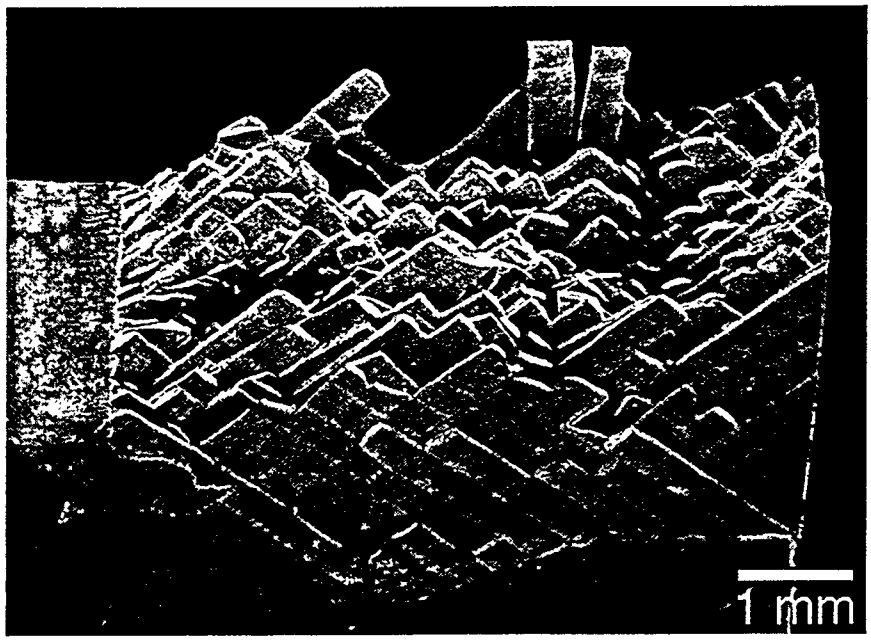

(b)

Fig. 7. Photomicrographs of fracture surfaces of notched (a) 0°/90° and (b) ±45° Si_3N_4/BN specimens; note increased tortuosity in (b).

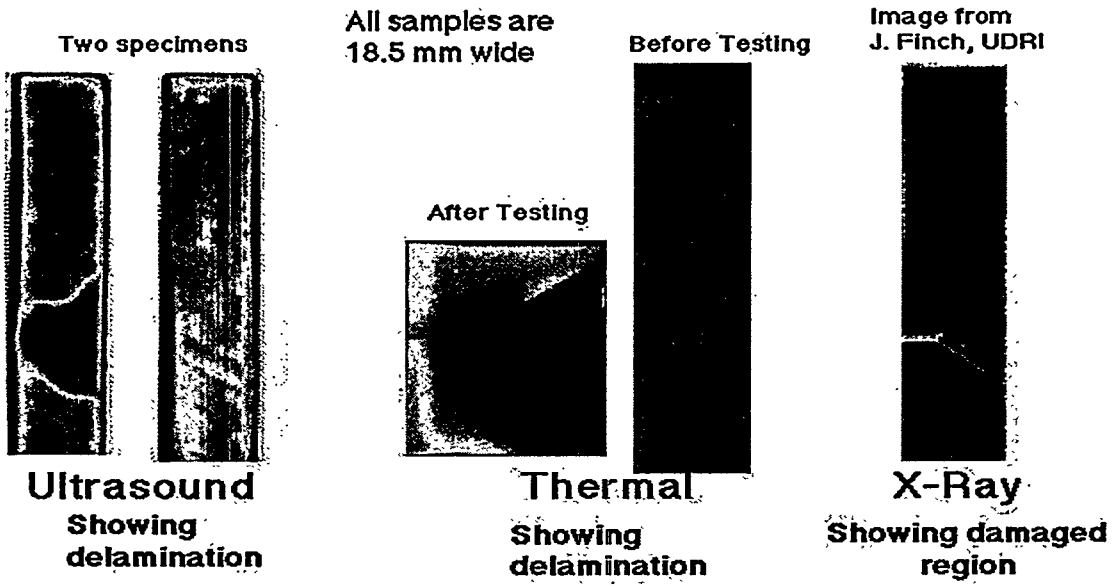

Fig. 8. Nondestructive examination data obtained on hand layup 0°/±45° Si_3N_4/BN FM: (a) through-transmission water-coupled ultrasound C-scan, (b) through-transmission thermal diffusivity, and (c) through-transmission microfocus X-ray with film detector [24].